Taylor & Francis
Taylor & Francis Group

RESEARCH PAPER

Check for updates

bHLH093/NFL and bHLH061 are required for apical meristem function in *Arabidopsis thaliana*

B. C. Poirier, M. J. Feldman [ORCID], and B. M. Lange [ORCID]

Institute of Biological Chemistry and M.J. Murdock Metabolomics Laboratory, Washington State University, Pullman, WA, USA

ABSTRACT

The basic Helix-Loop-Helix (bHLH) transcription factors SCREAM/ICE1 and SCREAM2 have well-characterized roles in the terminal differentiation of stomatal guard cells in *Arabidopsis thaliana*. Here we report on the characterization of the functional roles of the remaining members of sub-group IIIB, bHLH093 and bHLH061. The *bhlh093/bhlh061* double mutant failed to produce a primary inflorescence shoot and displayed greater phenotypic severity than *bhlh093* and *bhlh061* single mutants. An ultrastructural investigation revealed structural defects that develop in tissues surrounding the meristem prior to inflorescence emergence. The transition to flowering was restored in *bhlh093/bhlh061* with the application of gibberellin to the apex. We also demonstrate that gibberellin application alleviates structural defects that develop in tissues surrounding the meristem and restore meristem activity. Furthermore, the *bhlh093/bhlh061* double mutant was affected by delayed flowering, and the severity of the phenotype correlated with photoperiod and light intensity. Our results indicate that bHLH093 and bHLH061 function in the gibberellin-mediated establishment of functional apical meristems during the transition from vegetative to reproductive growth.

Introduction

Basic helix-loop-helix (bHLH) transcription factors harbor characteristic segments of 10–15 basic amino acids and two amphipathic α-helices separated by a variable loop region (about 40 amino acids). The basic region forms the main interface where contact with DNA occurs, whereas the two helices promote the formation of homo- or heterodimers between bHLH proteins, a prerequisite for DNA binding to occur.[1] bHLHs are ubiquitous throughout the Eukarya, where they form sizable gene families with, for example, 100–170 members in land plants. The *Arabidopsis thaliana* genome contains 133 bHLH genes, which are divided into 25 sub-groups.[2] The interaction with multiple partners endows bHLHs with the potential to function in a variety of capacities within different organs, tissues and cell types.

Two paralogous bHLHs of the sub-group IIIb, SCREAM/ICE1 (At3g26744) and SCREAM2 (At1g12860), act redundantly to coordinate cell fate transitions during stomatal development by forming heterodimers with SPCH, MUTE and FAMA.[3] The IIIb sub-group contains two additional genes, *bHLH093* (At5g65640) and *bHLH061* (At5g10570), which share high sequence identity with *SCREAM/ICE1* and *SCREAM2* in the DNA binding and ACT domains but lack conserved domains 4 and 6.[4] bHLH093 was identified as a potential interaction partner of FAMA through a bimolecular fluorescence complementation screen, but ectopic expression of *bHLH093* was reported to generate only a weak *fama* phenotype in a fraction of the plants investigated.[5] Because

bhlh093 mutants also do not display obvious defects in epidermal patterning,[5] it is likely that the predominant functions of bHLH093 and bHLH061 are not directly related to that of SCREAM/ICE1 and SCREAM2.

Sharma et al.[6] recently demonstrated that mutation of *bHLH093* leads to delayed flowering under short day conditions, with a corresponding decrease in gibberellin (GA) levels within apical tissues. Additionally, the transition to flowering in *bhlh093* mutants can be restored with exogenous GA application or upon crossing with a *della* quadruple mutant, indicating that bHLH093 likely functions upstream of GA signaling. GA promotes the transition to flowering in an FT-dependent pathway under long day and a separate FT-independent pathway under short day growth conditions, when FT expression is at low levels,[7] indicating that bHLH093 may function in the FT-independent, GA-mediated, transition to flowering.

The goal of the present study was to investigate whether bHLH093 may also have roles in floral transition under long day growth, and to further investigate the involvement of bHLH093 (and the thus far uncharacterized bHLH061) in floral transition. To this end, we evaluated the growth of *bhlh093*, *bhlh061* and *bhlh093/bhlh061* mutants under long day growth conditions with varying light intensities. We also investigated the developmental and ultrastructural changes prior to flowering to investigate the cause of delayed flowering in mutants. Here we present evidence that bHLH093 functions in conjunction with bHLH061 to facilitate the transition to flowering. The delay in

flowering in the *bhlh093/bhlh61* mutant was due to the development of structural defects that developed within tissues surrounding the shoot apical meristem prior to the establishment of an inflorescence meristem. These defects could be reversed by GA treatment. We also demonstrate that the severity of the flowering delay in the *bhlh093/bhlh61* mutant is dependent on both photoperiod and light intensity.

Results

Impaired expression of bhlh093 and bhlh061 causes several light intensity-dependent developmental defects

The T-DNA knock-out lines for *bHLH093* (termed *bhlh093-1* (within first exon), *bhlh093-2* (within first exon), *bhlh093-3* (upstream of coding sequence)) and *bHLH061* (termed *bhlh061-1* (within second intron), *bhlh061-2* (within third intron), *bhlh061-3* (upstream of coding sequence)) were PCR-analyzed to confirm the T-DNA insertion site (Figure 1A). A phenotypic analysis of all T-DNA insertion mutants and the *bhlh093-1/bhlh061-1* double-mutant showed no differences compared with wild-type controls under long day growth conditions with relatively low light intensities (90–120 µmol m^{-2} s^{-1}). However, under higher light intensities (150–250 µmol m^{-2} s^{-1}), *bHLH093* and *bHLH061* mutants were affected in several developmental characteristics, including a downward curling of rosette leaves (Supplemental Fig. 1) and impaired bolting and stem growth as compared with wild-type controls (Supplemental Fig. 2). The phenotypic appearance of the *bhlh093-1* and *bhlh093-2*
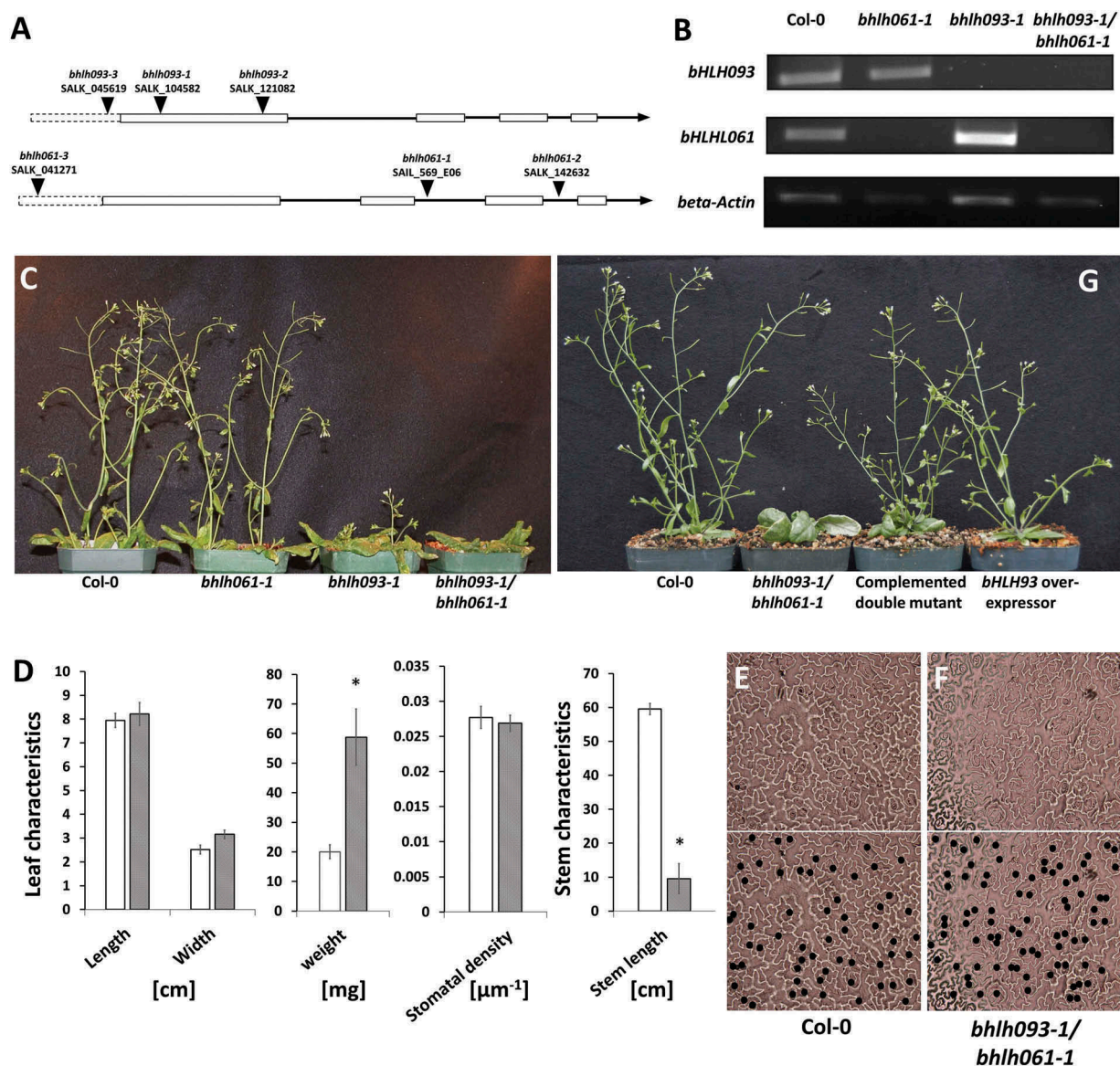

Figure 1. Phenotype of mutants impaired in the expression of bHLH transcription factors. **A** Intron-exon structure of the *bHLH093* and *bHLH061* genes in the Arabidopsis genome and location of T-DNA insertion sites. The box with dotted line indicates the promoter region. **B** RT-PCR with primers designed to amplify the *bHLH093* and *bHLH061* genes (note the absence of transcript for *bHLH093* in the *bhlh093-1* mutant, for *bHLH061* in the *bhlh061-1* mutant, and for both *bHLH093* and *bHLH061* in the *bhlh093-1/bhlh061-1* double mutant). **C** Delayed bolting phenotype in *bhlh* mutants (size bar 1 cm). **D** Biometric evaluation of *bhlh093-1/bhlh061-1* double mutant (striped bars) and wild-type controls (hollow bars) (standard deviation is indicated). Asterisks indicate P-value < 0.01 in a two-way ANOVA. There is no difference in the stomatal density on leaves of wild-type control (**E**) and the *bhlh093-1/bhlh061-1* double mutant (**F**). In the lower panels, black dots are added to indicate the position of stomata. **G** Transformation of the *bhlh093-1/bhlh061-1* double mutant with a functional copy of bHLH093 partially complements the bolting phenotype, while *bHLH093* overexpressors do not have an obvious phenotype (size bar 1 cm).

mutants was essentially identical, with *bhlh093-3* displaying less severe growth defects, and all further experiments were therefore performed with the *bhlh093-1* line as a representative allele (Supplemental Fig. 2). All *bhlh061* mutants displayed delayed bolting to varying degrees, and *bhlh061-1* was selected as the representative allele for future studies. Reverse transcription PCR confirmed the absence of bHLH093 and bHLH061 transcripts in the *bhlh093-1* and *bhlh061-1* lines (Figure 1B), respectively, thus confirming that these are transcript null alleles. To investigate a potential functional redundancy between bHLH093 and bHLH061, a cross was performed to generate a *bhlh093-1/bhlh061-1* double mutant, which was demonstrated to lack both the bHLH093 and bHLH061 transcripts (Figure 1B). The *bhlh093-1/bhlh061-1* double-mutant had a more severe phenotype than either of the single-mutants, exhibiting an almost complete loss of bolting (Figure 1C, D) and thicker rosette leaves (reflected in a significantly (2.9-fold) higher weight than in wild-type controls) (Figure 1D).

We then investigated if bHLH093 and bHLH061 may play roles in stomatal guard cell differentiation, akin to those demonstrated for their bHLH sub-group IIIb homologues, SCREAM/ICE1 and SCREAM2. No obvious effects of impaired expression of *bHLH093* alone were reported in a previous study,[5] and we thus focused on an analysis of stomata in mature rosette leaves of *bhlh093-1/bhlh061-1* double-mutant plants. The overall density of stomata was essentially identical in wild-type controls and mutants (Figure 1D). There was also no apparent clustering of stomata or aberrant cell division, which are characteristic of the *fama* loss-of-function phenotype, in the *bhlh093-1/bhlh061-1* mutant (Figure 1E, F). When the functional *bHLH093* allele was reintroduced into the *bhlh093-1/bhlh061-1* double mutant, the developmental defects were complemented, as indicated by a growth habitus with proper bolting and stem length similar to that of wild-type controls (Figure 1G). bHLH093 T2 overexpression lines had a phenotype similar to that of wild-type controls (Figure 1G).

The developmental characteristics of the *bhlh093-1/bhlh061-1* double mutant were then investigated in more detail. Compared to wild-type controls, the double mutant showed no significant differences in seed germination rates and etiolated and de-etiolated seedling growth at 10 d post-germination. Rosette leaf growth was also normal at 24 d after germination (Figure 2A). Phenotypic differences began to manifest when the primary inflorescence shoot emerged in wild-type controls (transition from growth stage 5.0 to 6.0 at 28 d after germination,[8] (Figure 2B). Besides delayed bolting, a severe downward curling of seemingly rough rosette leaves was the most striking phenotype observed with *bhlh093−1/bhlh061−1* mutant plants, while the appearance of cauline leaves in the double mutant was the same as in wild-type controls (Figure 2C, D). The emergence of small axillary inflorescences was not observed until approximately 52 d post-germination with the *bhlh093−1/bhlh061−1* mutants (Figure 2E) which is indicative of a loss of apical dominance. Rosette leaves of *bhlh093−1/bhlh061−1* plants entered senescence late, and small, greatly deformed, leaves continued to emerge under the original rosette even at 66 d after germination (Figure 2F).

Delayed flowering in the bhlh093-1/bhlh061-1 mutant is caused by impairment of meristem development

In Arabidopsis, the vegetative shoot apical meristem (SAM) transitions to an inflorescence meristem prior to bolting (the emergence of a primary inflorescence stem), which marks the transition to reproductive growth. Since *bhlh093−1/bhlh061−1* mutants fail to produce a primary inflorescence stem, a microscopic investigation was initiated to further evaluate defects in apical meristem function. Tissue was harvested just before bolting in wild-type controls (growth stage 5.0),[8] and serial sections were generated to explore meristem structure and organization. Based on observations made with longitudinal sections, the shoot apical meristem (SAM) in *bhlh093-1/bhlh061-1* mutants appeared to be severely curtailed (Figure 3A-C). When compared to wild-type controls, leaf primordia within the peripheral zone of mutant SAM were only barely visible. The typical dome structure of the SAM (as observed in wild-type controls) was also lacking in the double mutant. Further structural aberrations were observed in the region beneath the SAM. More specifically, a region of thickening growth was observed in *bhlh093-1/bhlh061-1* plants, with notably larger cells than in the corresponding wild-type controls (Figure 3A-C). Cross sections of *bhlh093-1/bhlh061-1* mutants at 40 d and 60 d post-germination revealed the presence of a cavity of increasing size within the center of rosettes, at a location where the SAM would be located prior to bolting in wild-type controls (Figure 3D, E).

Gibberellin application restores shoot apical meristem function in the bhlh093-1/bhlh061-1 double mutant

It is well established that hormones such as auxin, cytokinin and GA[9,10] are required for SAM function and maintenance. We thus applied these hormones directly to the shoot apex of the *bhlh093-1/bhlh061-1* mutant (untreated double mutants (Figure 4A) and wild-type (Figure 4B) as negative and positive controls, respectively). Administration of neither indole 3-acetic acid (auxin) nor N6-benzyl adenine (synthetic cytokinin) to the apical region rescued the mutant phenotype (Figure 4C), whereas treatment with 20 μM GA_3 (applied directly to the SAM every 24 h) partially rescued the bolting phenotype (Figure 4D). Interestingly, GA_3 treatment did not reverse the SAM to its typical dome shape (Figure 4E). In wild-type plants, GA_3 treatment promoted both early transition from a vegetative SAM to an inflorescence meristem and early growth of axillary meristems. No alterations in the structure of surrounding tissues were observed (Figure 4F).

Following up on the observation that GA_3 application to the apical region partially rescues the *bhlh093-1/bhlh061-1* mutant phenotype, we assessed if the impaired bolting was associated with a loss of apical dominance (central shoot tip is dominant over axillary bud outgrowth). We assessed apical dominance as the percentage of plants where the main stem grew more strongly than side stems. Apical dominance was 100% in wild-type controls but 0% in the double mutant. Apical dominance was restored in the double mutant with GA_3 treatment (100% at bolting) (Figure 5A). However, approximately 25% of mutant plants receiving GA_3 lost apical dominance at a later developmental stage (60 d post-germination), when one of the axillary stems surpassed the length of the primary inflorescence shoot.
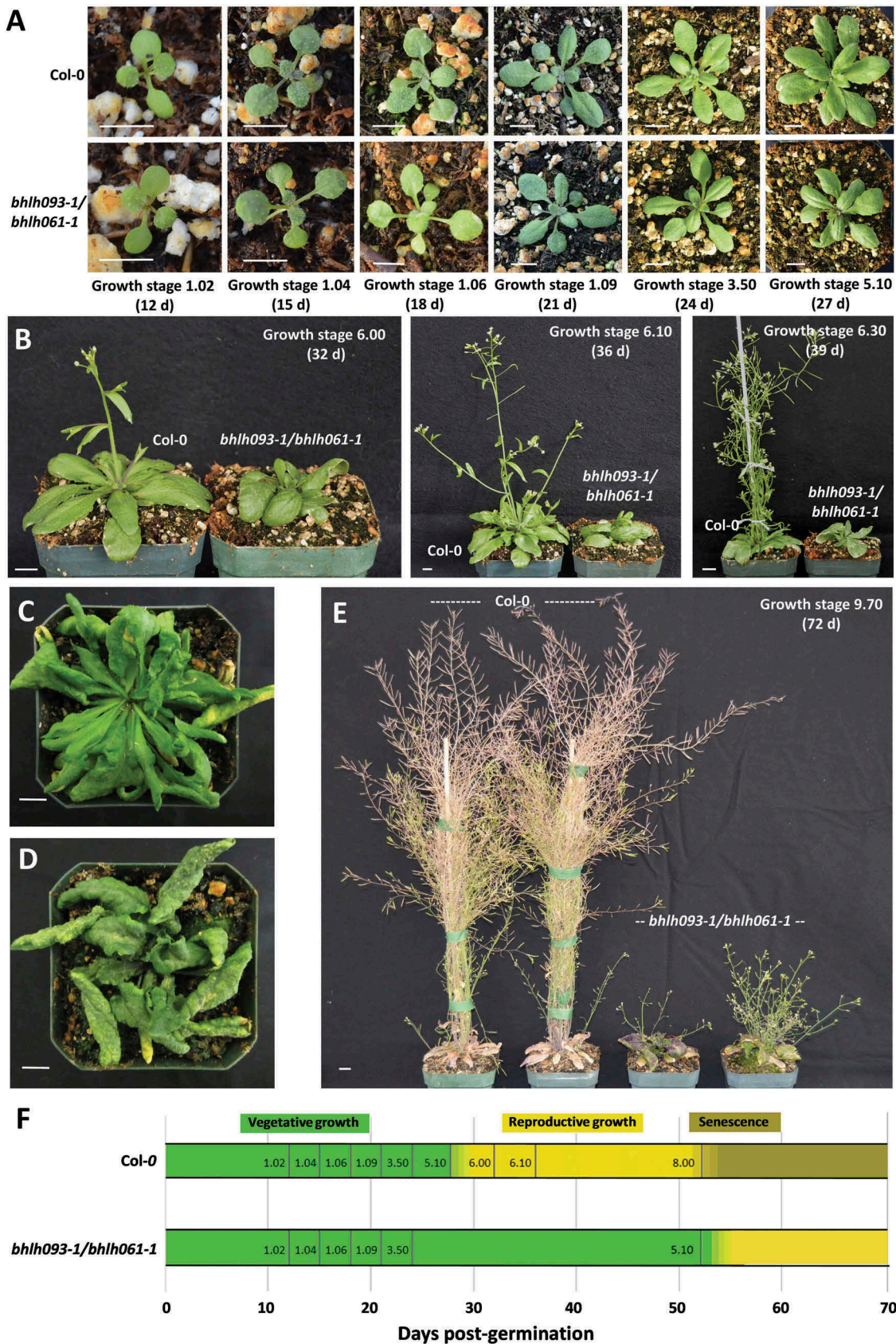
Figure 2. Emergence of phenotypic characteristics over a developmental time course. **A** Rosette leaves before bolting (growth stages 1.02 to 5.10 according to Boyes *et al.* 2001). **B** Lack of primary bolt in *bhlh093-1/bhlh061-1* double mutant. Wild-type control (**C**) and *bhlh093-1/bhlh061-1* double mutant (**D**) rosettes at 42 d post-germination (note the pronounced downward curling of double mutant leaves). **E** Phenotype of *bhlh093-1/bhlh061-1* double mutant at 72 d post-germination (inflorescences emerge only from axillary meristems; green leaves continue to emerge below the original rosette). **F** Scheme depicting the aberration of the developmental program in the *bhlh093-1/bhlh061-1* double mutant (compared to wild-type controls). The size bars for panels **A** – **E** correspond to 1 cm.

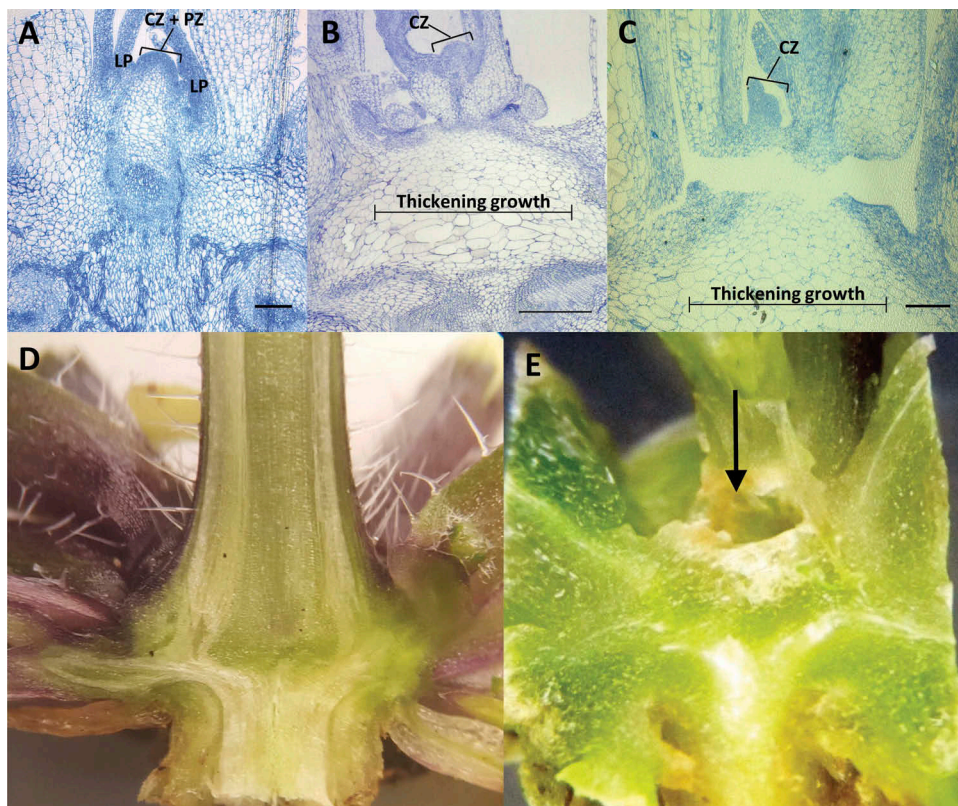**Figure 3.** Structural characteristics of the shoot apex. Longitudinal sections of the shoot apex) from wild-type control (**A**) and *bhlh093-1/bhlh061* double mutant (**B** and **C**) note the region of thickening growth below the meristem. Wild-type control (**D**) and bhlh093-1/bhlh061 double mutant (**E**) at 60 d post-germination. Note the cavity (arrow pointing toward it) located in the region beneath the SAM in the double mutant. Scale bars = 300 μm. Abbreviations: CZ, central zone; LP, leaf primordium; PZ, peripheral zone.

Leaf applications of GA$_3$ led to a partial rescue of apical dominance (about 50% at bolting) (Figure 5A). The severity of the bolting phenotype (loss of apical dominance) in the *bhlh093-1/bhlh061-1* mutant increased with the intensity of illumination and photoperiod length (Figure 5A). The timing of the transition from vegetative to reproductive growth, which was severely delayed in the *bhlh093-1/bhlh061-1* mutant, was re-established by GA$_3$ application (at both 20 μM and 100 μM) to the shoot apex (Figure 5B). However, the length of the primary inflorescence shoot remained about 30% shorter in the GA$_3$-treated double mutant when compared to wild-type controls (Figure 5C).

Discussion

Sub-group IIIb bHLH transcription factors are involved in controlling the functionality of meristems, but operate in different types of stem cells

The roles of *SCREAM/ICE1* and *SCREAM 2* in stomatal differentiation are well established.[3] *Promoter:GUS* assays, localization of GFP fusion proteins (expressed from native promoters) and cell type-specific transcriptome analyses all demonstrated a significantly enriched presence of SCREAM/ICE1 and SCREAM 2 in the stomatal cell lineage,[3,11] consistent with their functions in these cells. In contrast, the gene coding for bHLH093 (no previous data available for bHLH061), another sub-group IIIb member, is very highly expressed in the SAM[11–14] (Supplemental Fig. 3; expression level is comparable only in hypocotyl), which is consistent with the phenotype (loss of SAM functionality) reported

here. Based on analyses of fluorescence patterns obtained by expressing *bHLHL093:YFP* or *GFP:bHLH093* under control of the cauliflower mosaic virus 35S promoter, we and others demonstrated that bHLH093 localizes to nuclei (Supplemental Fig. 4),[6] which is in accordance with the subcellular localization reported for SCREAM/ICE1 and SCREAM 2.[3]

During the first 28 d post-germination under long-day growth conditions (16 h day/8 h night), the growth and development of rosette leaves occurred normally in a *bhlh093-1/bhlh061-1* loss-of-function mutant. However, at the time when bolting occurred in wild-type controls, the *bhlh093-1/bhlh061*-1 double mutant began to exhibit numerous defects. In particular, we observed a region of unusual thickening growth in the rib and elongation zones beneath the central zone of the SAM. Later in development (60 d post-germination), the SAM appeared to have been entirely aborted, thus leading to the formation of a cavity at the center of the rosette (Figure 3). Although the *bhlh093-1/bhlh061-1* mutant lacked a primary inflorescence shoot, axillary stems were produced late in development (starting on average at 52 d after germination), indicating a full loss of primary meristem function and impaired growth from axillary meristems in the axils of rosette leaves. Transformation of the *bhlh093-1/bhlh061-1* mutant with a constitutively expressed *bHLH093* copy led to a partial rescue towards wild-type phenotype (Figure 1), indicating that the defects are caused by impaired expression of *bHLH093* (with *bHLH061* as a secondary contributor to the phenotype).

In summary, the currently available evidence suggests that all members of the IIIb sub-group of bHLH transcription factors play
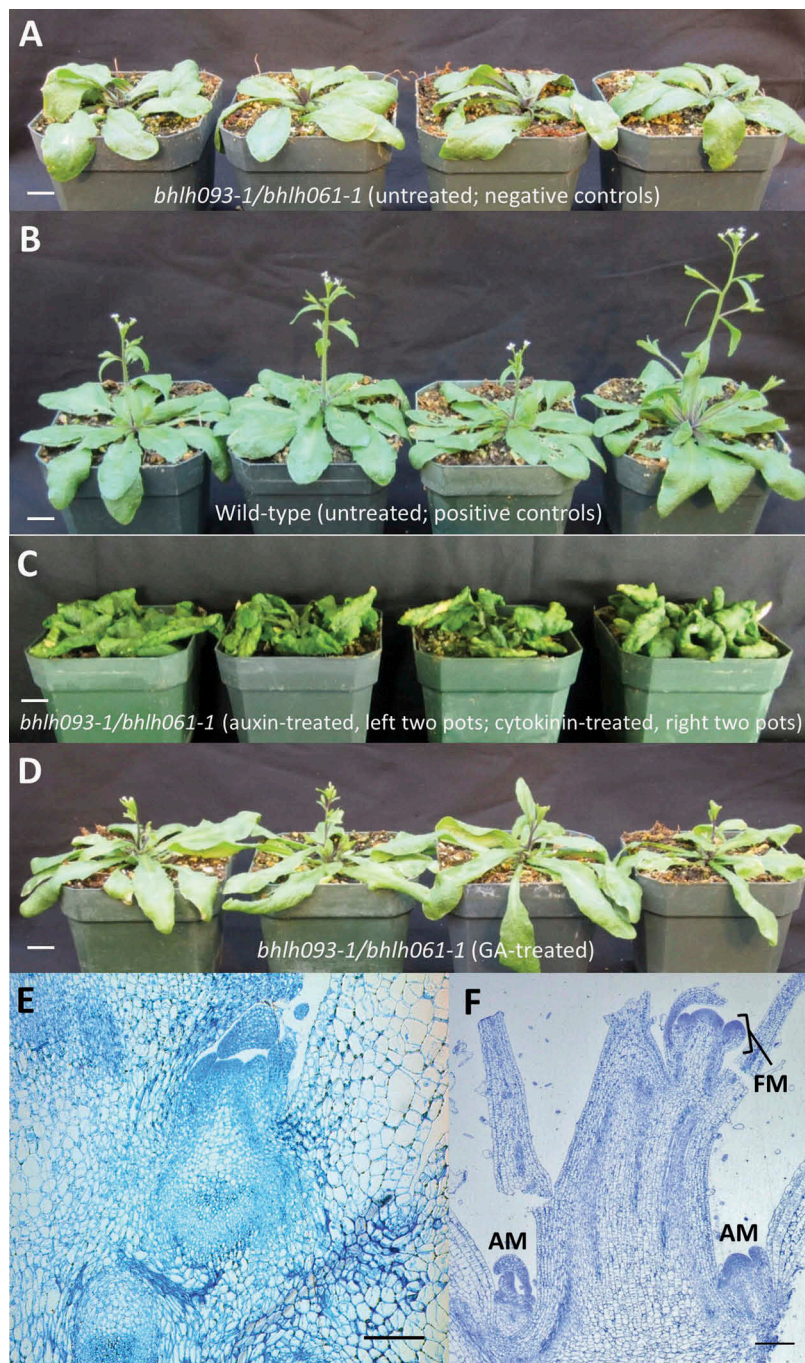
Figure 4. Application of gibberellin (GA$_3$) rescues the *bhlh093-1/bhlh061-1* double mutant toward a wild-type phenotype. Representative images of plants at 30 d post-germination. **A** untreated *bhlh093-1/bhlh061-1* double mutant (negative control); **B** mock-treated wild-type plants as positive controls; **C** *bhlh093-1/bhlh061-1* double mutant with SAM-applied auxin (left two pots) and cytokinin (right two pots) (note that these plants were photographed at 42 d post-germination (when severe curling occurs in wild-type plants as well) to test if a longer application may rescue the bolting phenotype); **D** *bhlh093-1/bhlh061-1* double mutant with SAM-applied GA$_3$. The size bars for panels **A** – **D** correspond to 1 cm. Microscopic images: GA$_3$ treatment of the *bhlh093-1/bhlh061-1* double mutant (applied to shoot apex) partially rescues the phenotype (**D**); GA$_3$ treatment of wild-type plants (**E**) leads to early development of inflorescence meristem and stem growth, as well as early initiation of axillary meristem growth. Scale bars = 300 µm. Abbreviations: AM, axillary meristem; FM, floral meristem.

important roles in determining the functionality of meristematic cells in *Arabidopsis*. However, while SCREAM/ICE1 and SCREAM 2 are required for proper differentiation of the stomatal stem cell lineage, we present evidence here that bHLH093 and bHLH061 have essential functions in maintaining the identity of SAM, indicating that the closely related subgroup IIIb bHLH proteins in *Arabidopsis* have evolved differential, cell type-specific roles in maintaining meristem function.

GA deficiency within the shoot apex is partly responsible for structural defects in bhlh093-1/bhlh061-1 *mutants, resulting in delayed flowering*

According to the classical model, the auxin indole 3-acetic acid is produced in the central zone of the shoot apex and then transported basipetally via polar auxin transport. Further down the stem it inhibits axillary bud growth by blocking cytokinin

A

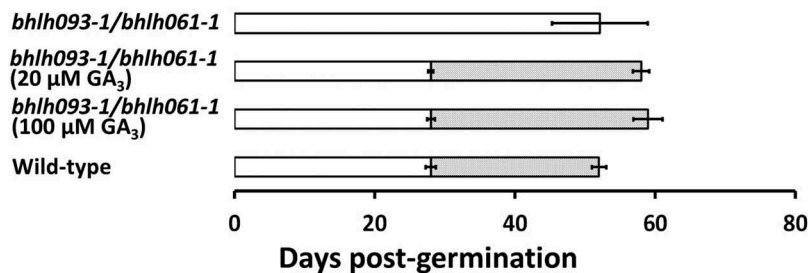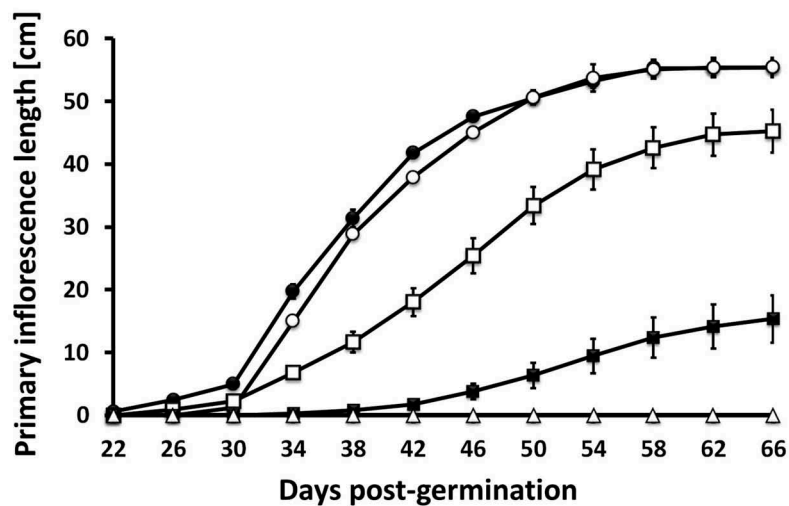| Genotype	Apical dominance [%]			
	Light intensity [μmol m^{-2} s^{-1}]			
	150	200	250	150
	Photoperiod (day/night [h])			
	16/8	16/8	16/8	24/0
Wild-type	100	100	100	100
bhlh093-1/bhlh61-1	44	34	0	0
bhlh093-1/bhlh61-1 (apex-applied GA$_3$)	–	–	100	–
bhlh093-1/bhlh61-1 (leaf-applied GA$_3$)	–	–	50	–

B

C

Figure 5. The *bhlh093-1/bhlh061-1* double mutant is affected by a light-dependent loss of apical dominance. **A** Apical dominance in as a function of light intensity and photoperiod. **B** Developmental time line of bolting and silique ripening (dotted bar; hollow bar indicates duration of vegetative growth) is restored by GA$_3$ application to the shoot apex (standard deviation is indicated for n = 6–8). **C** Time course of primary inflorescence shoot elongation in untreated wild-type controls (black circles), mock-treated wild-type controls (hollow circles), untreated *bhlh093-1/bhlh061* double mutant (hollow triangles), *bhlh093-1/bhlh061-1* double mutant with GA3 applied to the shoot apex (hollow squares), and *bhlh093-1/bhlh061-1* double mutant with GA3 applied to rosette leaves (black squares) (standard deviation is indicated for n = 3–4; note that some bars are smaller than symbols).

biosynthesis, thereby promoting growth of the primary stem.[15] However, cytokinin not only regulates the formation of axillary buds but also induces the expression of the master regulator *WUSCHEL* within the central zone of the SAM.[16] It is thus notable that our exogenous application of either hormone to the shoot tip had no effect on the impaired bolting phenotype in *bhlh093-1/bhlh061-1* loss-of-function plants. In contrast, exogenous application of GA$_3$ to the shoot apex was sufficient to restore bolting in *bHLH093-1/bHLH061-1* mutants (Figure 4).

This result may seem surprising, as it is generally accepted that gibberellin biosynthesis is repressed in the central zone, at

the level of GA 20-oxidase expression, by KNOTTED1-like homeobox (KNOX) transcription factors, thereby promoting meristematic activity.[17,18] It has further been established that KNOX proteins promote the transcription of the GA 2-oxidase gene, which encodes an enzyme responsible for gibberellin turnover to inactive forms of the growth regulator.[19,20] However, KNOX expression is comparatively low from the rib zone of the SAM and the elongation zone immediately beneath,[17,18] which coincides with relatively high transcript levels of the GA 3-β-hydroxylase gene (encoding the enzyme responsible for the formation of bioactive gibberellins) in these

cell types.[21] Interestingly, the defects caused by impaired expression of bHLH093/bHLH061 included enlarged cells in the rib meristem and elongation zone at the time when bolting occurred in wild-type controls. Later in development, the SAM was aborted and a cavity appeared in its place (Figure 3). Application of GA₃ was sufficient to partially rescue structural defects in bhlh093-1/bhlh061-1 plants, preventing atypical cell enlargement. We therefore hypothesize that GA₃ applied to the shoot tip was absorbed and then diffused to the rib and elongation zones, thereby restoring a gibberellin deficiency in the bhlh093-1/bhlh061-1 mutant. It further appears that KNOX activity was sufficient to maintain low gibberellin levels in the central zone and thus SAM functionality.

Progress toward understanding bhlh093 and bhlh061 function

Defective bolting, as observed with the bhlh093-1/bhlh061-1 mutant, is consistent with the lack of stem growth reported for gibberellin biosynthetic mutants,[22] and it is thus possible that bHLH093 and bHLH061 serve functions in regulating gibberellin biosynthesis in the shoot apex. Sharma et al.[6] reported that the gibberellin profile was affected significantly in the apex of bhlh093 mutant plants, which provides further support for the role of GA imbalances in producing the observed phenotype. However, insufficient GA supply in biosynthetic mutants results in leaves of dramatically reduced size[22] and not the increased biomass and substantial curling observed with the bhlh093-1/bhlh061-1 line. As an additional control experiment, we treated wild-type controls with the gibberellin biosynthesis inhibitor uniconazole-P (applied to shoot apex only) and observed the expected bolting phenotype but no visible effects on leaf shape (Supplemental Fig. 5). Uniconazole-P treatment of leaves causes growth retardation, as reported in numerous studies,[23] indicating that the leaf deformation of the bhlh093-1/bhlh061-1 line is unlikely to be caused directly by a defect in GA biosynthesis or perception in leaves.

The observation that GA₃ application to the shoot apex alleviates the bolting defect in the bhlh093-1/bhlh061-1 line indicates that the mutant is not impaired in GA perception. This assessment is further supported by the fact that a leaf application of GA₃ resulted in a partial rescue towards the wild-type bolting phenotype. The fact that only a partial rescue of the phenotype was achieved by treating leaves with GA₃ is likely a reflection of an inefficient uptake, long-distance transport from leaves to the shoot apex and/or subsequent recognition.[24–27] Interestingly, the leaf phenotype of the bhlh093-1/bhlh061-1 mutant (curling and increased biomass) was not rescued by GA₃ applications to the shoot apex or leaves. One might therefore hypothesize that the mutant is affected by a defect in GA perception in leaves. However, gibberellin-unresponsive mutants have a leaf phenotype (dwarf) similar to that of biosynthetic mutants,[28] and it would thus appear unlikely, as stated before, that the bhlh093-1/bhlh061-1 mutant is defective in gibberellin perception in leaves.

It was recently reported that bHLH093 is likely acting upstream of gibberellin signaling to promote flowering under short day conditions.[6] In that study, bhlh093 mutants failed to flower when grown under short day conditions (8h light/16h dark) with relatively high light intensity (200 μmol m^{-2} s^{-1}), but displayed normal growth under long day conditions (16h light/8h dark) with lower light intensity (120 μmol m^{-2} s^{-1}). Expression analysis of genes within apical tissues of a bhlh093 mutant at 60 days of growth (short day conditions) revealed decreased expression levels of GA biosynthetic genes (GA20ox1, GA3ox1 and GA3ox2) and increased expression of GA catabolic genes (GA2ox2 and GA2ox7).[6] Expanding on these previously established effects of bHLH093 on regulating GA biosynthesis, the data sets presented here indicate that the functions of the bHLH093 and bHLH061 transcription factors are contingent on both photoperiod and light intensity.

In Arabidopsis, GA is absolutely required for bolting, as indicated by observations with mutants defective in GA biosynthesis and perception, which are severely dwarfed, regardless of photoperiod.[29–31] An exception from this rule are mutants impaired in the expression of the GA response repressors GAI and RGA.[32] In contrast, flower initiation, which precedes bolting in Arabidopsis, is highly dependent on the photoperiod. Although the CONSTANS (CO)/FLOWERING LOCUS T (FT) pathway is generally thought to dominate under long day conditions, there is evidence that gibberellins may contribute to flower induction as well (in an FT-dependent and independent fashion).[33] While the relative importance of GA signaling for flower initiation is a matter of debate,[34] differences in light quality and intensity employed in experiments by different investigators may explain conflicting results.[33] This is consistent with our data, which document a light intensity-dependent bolting and flowering phenotype that is partially rescued by GA₃ applications to the apex or leaves.

While our observations and those of Sharma and colleagues[6] are not conflicting, our data allow us to present an updated interpretation for the primary role of bHLH093. In our model, bHLH093 and bHLH061 act partially redundant in the translation of a light intensity-dependent mobile signal that is required for the proper accumulation of GA in apical meristems, thereby supporting the transition to reproductive growth (Figure 6A). In bhlh093-1/bhlh061-1 mutant plants, gibberellin biosynthesis and catabolism are impaired under high light intensities, thus resulting in the failure to establish functional apical meristems. A secondary outcome of impaired bHLH093 and bHLH061 expression is that, when reproductive growth cannot be established, another mobile signal affects processes that lead to the downward curling leaf phenotype, increased vegetative growth and a delay in leaf senescence (Figure 6B). This phenotype is reminiscent of that reported for plants in which the shoot apex or reproductive organs have been removed, which leads to a disruption in source – sink relationships (demonstrated in soybean,[35] Arabidopsis,[36] wheat,[37] and cotton[38]). The gene targets of the bHLH093 and bHLH061 transcription factors, and their relationship to light intensity, are as yet unknown, and pursuing these mechanistic questions will now be highly instructive.
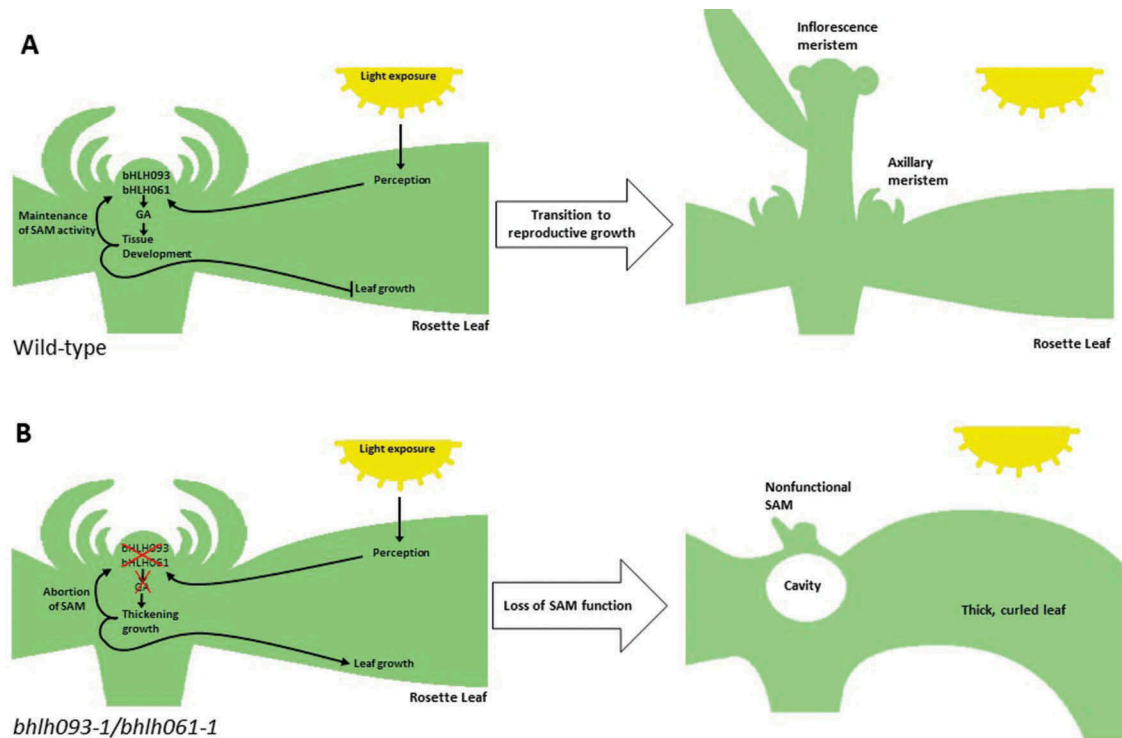
Figure 6. Proposed model of bHLH093/bHLH061 function. **A** bHLH093 and bHLH061 act upstream of GA signaling within the apex, integrating a light intensity-dependent signal to regulate growth within the apex and promote the transition to flowering. **B** Loss of bHLH093/bHLH061 function leads to a decrease in endogenous GA levels, disrupting tissue development and resulting in the termination of the SAM. Delayed transition to reproductive growth causes aberrant rosette leaf growth as a secondary effect.

Materials and methods

Selection of homozygous T-DNA insertion lines

T-DNA insertion lines bhlh093-1 (SALK_104582), bhlh093-2, (SALK_121082), bhlh093-3 (SALK _045619), bhlh061-1 (SAIL_569_E06), bhlh061-2 (SALK_142632) and bhlh061-3 (SALK_041271) were obtained from the Arabidopsis Biological Resource Center (ABRC).[39] PCR genotyping was performed to confirm that the T-DNA insertion lines obtained from ABRC were homozygous for the T-DNA insertion allele. Genotyping was again used to identify segregation patterns in an F2 T-DNA insertion population generated through genetic crosses between bhlh093-1 and bhlh061-1 homozygotes. Oligonucleotide primers were designed using the Signal T-DNA server (http://signal.salk.edu/cgi-bin/tdnaexpress) to assess the allele state at T-DNA insertion sites: bHLH093-1F, 5′-TTTTCGATGGACGAATCTGTC-3′, bHLH093-1R, 5′-TACTGATTTTTGGGACGATGG-3′ and bHLH061, F, 5′-GATTAGAAACCGAGGGGTCAG-3′, bHLH061R, 5′- AAGGTCAGCCTTCGAAGAATC-3′, SALK lines; LBa1, 5′- TGGTTCACGTAGTGGGCCATCG-3′, SAIL lines; SAILLB1 5′- GCCTTTTCAGAAATGGATAAATAGCCTTGCTTCC-3′. The following primers were used to assess transcript presence/absence by Reverse Transcription Polymerase Chain Reaction (RT-PCR): bHLH93RT-PCRF1, 5′-GGATTTGATCATCATCATCATCA-3′; bHLH93RT-PCRR1, 5′-ACTGAACTCATAATGTTTTCCCCTA-3′; bHLH61RT-PCR-F1, 5′-CTCATCTAAGCACCCTCATTACA-3′; bHLH61-RT-PCR-R1, ATCTCCTTATGAAATATCATACT-3′. Taq polymerase (New England Biolabs, Ipswich, MA, USA) was used to perform gene fragment

amplifications. PCR cycling conditions were: initial denaturation at 94°C for 2 min; 40 cycles of 94°C for 30 s, 55°C for 20 s and 72°C for 90 s; and final extension for 5 min at 72°C.

Bhlh093 overexpression and complementation

An open reading frame (ORF) clone of bHLH093 (stock #U82500) was obtained from ABRC and amplified in High-Fidelity PCR Master Mix (Finnzymes, Waltham, MA, USA) using the following oligonucleotides: bHLH093FL-L, 5′ AAAAAGCAGGCTCCACCATGGAACTGTCGACTCAAAT-3′, bHLH093FL-R, 5′- AGAAAGCTGGGTCTTACAAGCAGCTTCCACCAT-3′. PCR was used to incorporate Gateway recombination sites onto the ORF using the following primers; ATTBL, 5′- GGGGACAAGT TTGTACAAAAAAGCAGGCT −3′, and ATTBR, 5′- GGGGACCACTTTGTACAAGAAAGCTGGGT −3′. The ORF fragment was then cloned into the pDONR221 vector using a Gateway BP Clonase (Invitrogen, Carlsbad, CA, USA) reaction. DNA sequencing using M13F and M13R primers was used to verify the sequence of this construct before an LR reaction was employed to clone the bHLH093 ORF into the plant expression vector pH7WG2.[40] The bHLH093 overexpression construct was transformed into Agrobacterium tumefaciens strain GV3101 by electroporation, which was then used to transform Arabidopsis Col-0 wild-type and the bhlh093-1/bhlh061-1 double knock-out line by the floral dipping method.[41] Selection of homozygous transformants was achieved through plating of seeds on half-strength MS media containing 0.95% (w/v) agar and 20 µg mL^{-1} hygromycin.

Intracellular localization of bhlh093

The coding sequence of *bHLH093* was amplified as described above and cloned into the pDONR/Zeo vector using a Gateway BP (Invitrogen, Carlsbad, CA, USA) reaction. Following sequence verification, the coding sequence of bHLH093 was then transferred into the pMDC43 vector by a Gateway LR reaction, thus creating an N-terminal *GFP: bHLH093* fusion construct. Gold particles (1 μm diameter) were coated with 0.5 μg of plasmid DNA containing the *GFP: bHLH093* construct (or pMDC43 vector alone as a negative control) and bombarded into onion epidermal peel cells with a helium-gas-driven particle accelerator (PDS-1000/He; Bio-Rad, Hercules, CA, USA) operated at a pressure of 76 bar and a chamber vacuum of 0.8 bar. Samples were kept at 25°C in darkness for 24 h and fluorescence was observed by fluorescence microscopy data using a LSM 510 META Confocal microscope (Zeiss, Thornwood, NY, USA).

Biomass measurements and other phenotyping

Seeds were moved to a dark cold room (4°C) for 2 weeks to break dormancy, sterilized with two wash steps using 96% ethanol and one wash step consisting of 20% (v/v) hypochlorite and 0.1% Tween-20, and rinsed five times with sterile water. The seeds were then spread onto plates containing 1% (w/w) agar in half-strength MS salts and stored in the dark for 2 d. An LI-189 light meter (LI-COR, Lincoln, NE, USA) was used to measure photosynthetic photon fluence rate over the waveband 400–700 nm, hereby referred to as "light intensity". Following determination of seed germination rates, plates were moved into a growth chamber (16 h day/8 h night cycle; 250 μmol m^{-2} s^{-1} light intensity; 24°C; 70% humidity) and seedling growth was assessed for 7 d. Alternatively, seeds were germinated in 75-mm pots on Sunshine professional growing mix and maintained under the same growth conditions as listed above. For biomass measurements, the three largest rosette leaves were harvested from each plant at 42 d after germination and placed in an oven at 50°C for 7 d to ensure complete desiccation. Two developmental checkpoints (growth stages as defined previously)[8] were employed to obtain information about the life-cycle progression of mutants: (1) bolting (transition from growth stage 5.0 to 5.1) and (2) silique ripening (growth stage 8.00 (first silique shattered)). Measurements of stem height were performed every 4 d by recording the length of the primary stem and longest axillary stem for each plant. Plants with an axillary stem of greater length than the primary stem were considered to have lost apical dominance.

Stomatal density was calculated based on a morphometric analysis of light microscopic images. Epidermal peels were generated by coating the abaxial leaf surface of the second longest leaf with top coat nail polish (Sephora, Paris, France), air-drying for 5 min and removing impressions with Scotch sealing tape (3M, Maplewood, MN, USA). The impressions were then mounted on slides and viewed under a DMLB fluorescent microscope (Leica, Wetzlar, Germany). Photos at 200-fold magnification were taken with an Eos Rebel T5 camera (Canon, Tokyo, Japan) and analyzed using ImageJ software (National Institute of Health). Leaf areas were calculated by calibration of ImageJ using a stage micrometer.

Microscopy

To examine meristem topology leading up to flowering, rosettes were harvested at 12, 15 and 17 days of growth from wild-type, *bhlh093-1/bhlh061-1*, and GA-treated *bhlh093-1/bhlh061-1* plants (100 μM GA_3 applied every 4 d to meristem). Rosettes were dissected to remove young developing leaves, exposing the meristem at the center. Samples were mounted on stubs with carbon tape and visualized using a Quanta Environmental Scanning Electron Microscope (FEI, Hillsboro, OR, USA) under low vacuum and 20 kV accelerating voltage. To investigate the properties of the meristem region leading up to flowering, entire rosettes were harvested prior to the establishment of an inflorescence meristem. Rosettes were held upside-down and a razor blade was used to remove the leaves by cutting the petioles along the axis of the primary root. The approximately 2 mm wide tissue fragment remaining at the center of the original rosette, which contained the SAM, was dissected in half along the vertical axis with an ultra-sharp razor blade and the two halves were fixed and embedded separately. The fixation was performed with formalin–acetic acid–alcohol (50% (v/v) ethanol, 5 % (v/v) acetic acid, and 3.7% (v/v) formaldehyde in water) using three rounds of vacuum infiltration (1.4 bar for 20 min each round). The samples were then embedded in Spurr's resin according to existing protocols,[42] using ethanol for tissue dehydration and acetone as the intermediate solvent for resin infiltration. Embedded samples were sectioned to a thickness of 700 nm using an ultra-cut microtome (Reichert-Jung, Wien, Austria). Serial sections were generated to facilitate navigation through the Z-axis of the plant tissue, ensuring that the section obtained was centered within the meristem region. Sections were then transferred to gelatin-coated microscope slides, air-dried for 10 min, and stained with 0.1% (w/v) toluidine blue and 1% (w/v) sodium borate in water. An Aristoplan light microscope (Leitz, Wetzlar, Germany) was used to view sections and a DFC 425C camera (Leica Biosystems, Buffalo Grove, IL, USA) employed to capture photographic images. Scale bars were added using ImageJ software (National Institutes of Health).

Hormone and inhibitor applications

Plants were grown in 75-mm pots under a 16 h light/8 h dark cycle, with high pressure sodium lamps (250 μmol m^{-2} s^{-1}) as primary light source. Chemical treatments were performed at 3 PM on experimental days. Experiment 1: wild-type positive controls (Col-0 ecotype) and *bHLH093-1/bHLH061-1* negative controls received no chemical treatment; benzyl adenine (synthetic cytokinin) treatments (direct application to shoot apex with mutant plants only): (1) 30 μL of a 50 μM solution in water, applied every 2 d; (2) 30 μL of a 150 μM solution in water, applied every 2 d. Experiment 2: wild-type positive controls (Col-0 ecotype) and *bHLH093-1/bHLH061-1* negative controls received no chemical treatment; indole 3-acetic acid (auxin) treatments (direct application to shoot apex with mutant plants only): (1) 30 μL of a 5 μM solution in water, applied every 2 d directly to shoot apex; (2) 30 μL of a 50 μM

solution in water, applied every 2 d. Experiment 3: wild-type positive controls (Col-0 ecotype) and *bHLH093-1/bHLH061-1* negative controls received a mock treatment of shoot apex-applied 0.1% (v/v) Tween-80 and GA$_3$ (bioactive gibberellin): (1) 30 μL of a 20 μM GA$_3$ solution in 0.1% (v/v) Tween-80, applied every 24 h directly to shoot apex; (2) 30 μL of a 100 μM GA$_3$ solution in 0.1% (v/v) Tween-80, applied every 4 d directly to shoot apex; (3) 100 μL of a 100 μM GA$_3$ solution in 0.1% (v/v) Tween-80, applied to leaves with a brush every 4 d. Experiment 4: wild-type positive controls (Col-0 ecotype) and *bHLH093-1/bHLH061-1* negative controls received a mock treatment of shoot apex-applied 0.05% (v/v) Tween-80; uniconazol-P (gibberellin biosynthesis inhibitor) treatments (wild-type plants only): (1) 30 μL of a 10 μM solution in 0.05% (v/v) Tween-80, applied daily directly to shoot apex; (2) 30 μL of a 1 μM solution in 0.05% (v/v) Tween-80, applied daily directly to shoot apex.

Disclosure of potential conflicts of interest

The authors declare that they have no competing interests.

Funding

Author biographies

B.C.P., M.J.F. and B.M.L. conceived of the experimental strategy. B.C.P. and M.J.F. performed all experiments. B.C.P., M.J.F. and B.M.L. analyzed data. B.M.L. wrote the manuscript, with input from B.C.P. and M.J.F.

ORCID

M. J. Feldman 🔾 http://orcid.org/0000-0002-5415-4326
B. M. Lange 🔾 http://orcid.org/0000-0001-6565-9584

References

1. Jones S. An overview of the basic helix-loop-helix proteins. Genome Biol. 2004;5:226. doi:10.1186/gb-2004-5-6-226.
2. Buck MJ, Atchley WR. Phylogenetic analysis of plant basic helix-loop-helix proteins. J Mol Evol. 2003;56:742─750. doi:10.1007/s00239-002-2449-3.
3. Kanaoka MM, Pillitteri LJ, Fujii H, Yoshida Y, Bogenschutz NL, Takabayashi J, Zhu JK, Torii KU. SCREAM/ICE1 and SCREAM2 specify three cell-state transitional steps leading to Arabidopsis stomatal differentiation. Plant Cell. 2008;20:1775─1785. doi:10.1105/tpc.108.060848.
4. Pires N, Dolan L. Origin and diversification of basic-helix-loop-helix proteins in plants. Mol Biol Evol. 2010;27:862─874. doi:10.1093/molbev/msp288.
5. Ohashi-Ito K, Bergmann DC. Arabidopsis FAMA controls the final proliferation/differentiation switch during stomatal development. Plant Cell. 2006;18:2493─2505. doi:10.1105/tpc.106.046136.
6. Sharma N, Xin R, Kim DH, Sung S, Lange T, Huq E. NO FLOWERING IN SHORT DAY (NFL) is a bHLH transcription factor that promotes flowering specifically under short-day conditions in Arabidopsis. Development. 2016;143:682─690. doi:10.1242/dev.128595.
7. Hisamatsu T, King RW. The nature of floral signals in Arabidopsis. II. Roles for FLOWERING LOCUS T (FT) and gibberellin. J Exp Bot. 2008;59:3821─3829. doi:10.1093/jxb/ern232.
8. Boyes DC, Zayed AM, Ascenzi R, McCaskill AJ, Hoffman NE, Davis KR, Görlach J. Growth stage-based phenotypic analysis of Arabidopsis: a model for high throughput functional genomics in plants. Plant Cell. 2001;13:1499─1510.
9. Shani E, Yanai O, Ori N. The role of hormones in shoot apical meristem function. Curr Op Plant Biol. 2006;9:484─489. doi:10.1016/j.pbi.2006.07.008.
10. Murray JA, Jones A, Godin C, Traas J. Systems analysis of shoot apical meristem growth and development: integrating hormonal and mechanical signaling. Plant Cell. 2012;24:3907─3919. doi:10.1105/tpc.112.098962.
11. Schmid M, Davison TS, Henz SR, Pape UJ, Demar M, Vingron M, Schölkopf B, Weigel D, Lohmann JU. A gene expression map of Arabidopsis thaliana development. Nature Genet. 2005;37:501─506. doi:10.1038/ng1495.
12. Toufighi K, Brady SM, Austin R, Ly E, Provart NJ. The botany array resource: e-northerns, expression angling, and promoter analyses. Plant J. 2005;43:153─163. doi:10.1111/j.1365-313X.2005.02437.x.
13. Winter D, Vinegar B, Nahal H, Ammar R, Wilson GV, Provart NJ. An "electronic fluorescent pictograph" browser for exploring and analyzing large-scale biological data sets. PloS One. 2007;2: e718. doi:10.1371/journal.pone.0000718.
14. Yadav RK, Tavakkoli M, Xie M, Girke T, Reddy GV. A high-resolution gene expression map of the Arabidopsis shoot meristem stem cell niche. Development. 2014;141:2735─2744. doi:10.1242/dev.106104.
15. Müller D, Leyser O. Auxin, cytokinin and the control of shoot branching. Ann Bot. 2011;107:1203─1212. doi:10.1093/aob/mcr069.
16. Gordon SP, Chickarmane VS, Ohno C, Meyerowitz EM. Multiple feedback loops through cytokinin signaling control stem cell number within the Arabidopsis shoot meristem. Proc Natl Acad Sci USA. 2009;106:16529─16534. doi:10.1073/pnas.0908122106.
17. Sakamoto T, Kamiya N, Ueguchi-Tanaka M, Iwahori S, Matsuoka M. KNOX homeodomain protein directly suppresses the expression of a gibberellin biosynthetic gene in the tobacco shoot apical meristem. Genes Dev. 2001;15:581─590. doi:10.1101/gad.867901.
18. Hay A, Kaur H, Phillips A, Hedden P, Hake S, Tsiantis M. The gibberellin pathway mediates KNOTTED1-type homeobox function in plants with different body plans. Curr Biol. 2002;12:1557─1565. doi:10.1016/S0960-9822(02)01125-9.
19. Sakamoto T, Kobayashi M, Itoh H, Tagiri A, Kayano T, Tanaka H, Iwahori S, Matsuoka M. Expression of a gibberellin 2-oxidase gene around the shoot apex is related to phase transition in rice. Plant Physiol. 2001;125:1508─1516.
20. Jasinski S, Piazza P, Craft J, Hay A, Woolley L, Rieu I, Phillips A, Hedden P, Tsiantis M. KNOX action in Arabidopsis is mediated by coordinate regulation of cytokinin and gibberellin activities. Curr Biol. 2005;15:1560─1565. doi:10.1016/j.cub.2005.07.023.
21. Itoh H, Tanaka-Ueguchi M, Kawaide H, Chen XB, Kamiya Y, Matsuoka M. The gene encoding tobacco gibberellin 3 beta-hydroxylase is expressed at the site of GA action during stem elongation and flower organ development. Plant J. 1999;20:15─24. doi:10.1046/j.1365-313X.1999.00568.x.
22. Yamaguchi S. Gibberellin metabolism and its regulation. Annu Rev Plant Biol. 2008;59:225─251. doi:10.1146/annurev.arplant.59.032607.092804.
23. Rademacher W. GROWTH RETARDANTS: effects on gibberellin biosynthesis and other metabolic pathways. Annu Rev Plant Physiol Plant Mol Biol. 2000;51:501─531. doi:10.1146/annurev.arplant.51.1.501.
24. Reid JB. Internode length in Pisum: do the internode length genes effect growth in dark-grown plants? Plant Physiol. 1983;72:759─763.

25. Proebsting WM, Hedden P, Lewis MJ, Croker SJ, Proebsting LN. Gibberellin concentration and transport in genetic lines of pea: effects of grafting. Plant Physiol. 1992;100:1354–1360.

26. Eriksson S, Bohlenius H, Moritz T, Nilsson O. GA4 is the active gibberellin in the regulation of LEAFY transcription and Arabidopsis floral initiation. Plant Cell. 2006;18:2172–2181. doi:10.1105/tpc.106.042317.

27. Ueguchi-Tanaka M, Nakajima M, Katoh E, Ohmiya H, Asano K, Saji S, Hongyu X, Ashikari M, Kitano H, Yamaguchi I, et al. Molecular interactions of a soluble gibberellin receptor, GID1, with a rice DELLA protein, SLR1, and gibberellin. Plant Cell. 2007;19:2140–2155. doi:10.1105/tpc.106.043729.

28. Daviere JM, Achard P. Gibberellin signaling in plants. Development. 2013;140:1147–1151. doi:10.1242/dev.087650.

29. Griffiths J, Murase K, Rieu I, Zentella R, Zhang ZL, Powers SJ, Gong F, Phillips AL, Hedden P, Sun TP, et al. Genetic characterization and functional analysis of the GID1 gibberellin receptors in Arabidopsis. Plant Cell. 2006;18:3399–3414. doi:10.1105/tpc.106.047415.

30. Koornneef M, Vanderveen JH. Induction and analysis of gibberellin sensitive mutants in Arabidopsis thaliana (L) Heynh. Theor Appl Genet. 1980;58:257–263. doi:10.1007/BF00265176.

31. Rieu I, Ruiz-Rivero O, Fernandez-Garcia N, Griffiths J, Powers SJ, Gong F, Linhartova T, Eriksson S, Nilsson O, Thomas SG, et al. The gibberellin biosynthetic genes AtGA20ox1 and AtGA20ox2 act, partially redundantly, to promote growth and development throughout the Arabidopsis life cycle. Plant J. 2008;53:488–504. doi:10.1111/j.1365-313X.2007.03360.x.

32. King KE, Moritz T, Harberd NP. Gibberellins are not required for normal stem growth in Arabidopsis thaliana in the absence of GAI and RGA. Genetics. 2001;159:767–776.

33. King RW, Hisamatsu T, Goldschmidt EE, Blundell C. The nature of floral signals in Arabidopsis. I. Photosynthesis and a far-red photoresponse independently regulate flowering by increasing expression of FLOWERING LOCUS T (FT). J Exp Bot. 2008;59:3811–3820. doi:10.1093/jxb/ern231.

34. Mutasa-Göttgens E, Hedden P. Gibberellin as a factor in floral regulatory networks. J Exp Bot. 2009;60:1979–1989. doi:10.1093/jxb/erp040.

35. Crafts-Brandner SJ, Egli DB. Sink removal and leaf senescence in soybean. Plant Physiol. 1987;85:662–666.

36. Ye Z, Rodriguez R, Tran A, Hoang H, De Los Santos D, Brown S, Vellanoweth RL. The developmental transition to flowering represses ascorbate peroxidase activity and induces enzymatic lipid peroxidation in leaf tissue in Arabidopsis thaliana. Plant Sci. 2000;158:115–127. doi:10.1016/S0168-9452(00)00316-2.

37. Srivalli B, Khanna-Chopra R. The developing reproductive 'sink' induces oxidative stress to mediate nitrogen mobilization during monocarpic senescence in wheat. Biochem Biophys Res Commun. 2004;325:198–202. doi:10.1016/j.bbrc.2004.10.013.

38. Dong H, Niu Y, Kong X, Luo Z. Effects of early-fruit removal on endogenous cytokinins and abscisic acid in relation to leaf senescence in cotton. Plant Growth Regul. 2009;59:93–101. doi:10.1007/s10725-009-9392-x.

39. Alonso JM, Stepanova AN, Leisse TJ, Kim CJ, Chen H, Shinn P, Stevenson DK, Zimmerman J, Barajas P, Cheuk R, et al. Genome-wide insertional mutagenesis of Arabidopsis thaliana. Science. 2003;301:653–657. doi:10.1126/science.1086391.

40. Curtis MD, Grossniklaus U. A gateway cloning vector set for high-throughput functional analysis of genes in planta. Plant Physiol. 2003;13:462–469.

41. Clough SJ, Bent AF. Floral dip: a simplified method for Agrobacterium-mediated transformation of Arabidopsis thaliana. Plant J. 1998;16:735–743. doi:10.1046/j.1365-313x.1998.00343.x.

42. Wu S, Baskin TI, Gallagher KL. Mechanical fixation techniques for processing and orienting delicate samples, such as the root of Arabidopsis thaliana, for light or electron microscopy. Nature Prot. 2012;7:1113–1124. doi:10.1038/nprot.2012.056.